




Age-dependent copy number variations of TP53 tumour suppressor gene associated with altered phosphorylation status of p53 protein in sporadic schwannomas

Hongsai Chen^{1,2,3,4} · He Huang^{1,2,3} · Jingjing Zhao^{1,2,3} · Zhigang Wang^{1,2,3} · Mengling Chang⁵ · Lu Xue^{1,2,3} · Weidong Zhu^{1,2,3} · Yongchuan Chai^{1,2,3} · Gen Li^{1,2,3} · Zhaoyan Wang^{1,2,3}  · Hao Wu^{1,2,3}

Received: 23 February 2019 / Accepted: 25 April 2019 / Published online: 2 May 2019
© Springer Science+Business Media, LLC, part of Springer Nature 2019

Abstract

Purpose Point mutations of *TP53* tumour suppressor are very rare in schwannomas. We aim to characterize the frequency of exonic copy-number changes of the gene in the tumour and to examine the association between *TP53* alterations, phosphorylation status of p53 protein and clinical phenotypes.

Methods The alterations of *TP53* were screened by a combination of Sanger sequencing and multiplex ligation-dependent probe amplification (MLPA) in a total of 44 vestibular schwannomas. The mutation index (MI) in a tumour was defined as the number of exons mutated/ the number of exons tested. Phosphorylation status of p53 protein was investigated by immunoblotting and immunofluorescence.

Results MLPA analysis showed single and multi-exon deletion mutations of *TP53* in 65.7% of the cases. Comparisons of clinical features between mutated and non-mutated patients established an association of *TP53* mutations with progressive phenotypes, including an earlier formation and a larger tumour. In addition, there were significant correlations between MI and both patients' age and tumour size. The Ser 392 phosphorylation level of p53 varied among tumours, and correlation analysis revealed an age-dependent phosphorylation pattern. The majority of tumours with hyperphosphorylated p53 were from mutated and young patients, suggesting an association of Ser392 phosphorylation with the mutational status of *TP53* involved in the acceleration of tumour growth in young individuals. Moreover, Ser 392 phosphorylation contributed to a nuclear accumulation of p53 in schwannoma cultures with *TP53* mutation.

Conclusions An interplay between the mutation status of *TP53*, phosphorylation patterns and tumour behaviors might be established in the disease.

Keywords Schwannomas · TP53 · Mutation · Phosphorylation

Hongsai Chen, He Huang, Jingjing Zhao and Zhigang Wang contributed equally to this work.

Electronic supplementary material The online version of this article (<https://doi.org/10.1007/s11060-019-03176-1>) contains supplementary material, which is available to authorized users.

✉ Zhaoyan Wang
wzyent@126.com

✉ Hao Wu
wuhao622@sina.cn

Extended author information available on the last page of the article

Introduction

Vestibular schwannomas (VSs) are benign, slowly growing encapsulated neoplasms originating from the Schwann cell sheath surrounding the vestibular branch of cranial nerve VIII. Regarding VSs, their frequency of occurrence is rather high in comparison with schwannomas at other regions in the head and neck. Although they are benign, their location inside the internal auditory canal and growth into the cerebellopontine angle make management difficult, and patients experience significant morbidity and mortality. The great majority of VSs are sporadic and unilateral schwannomas, which usually develop between ages 40 and 60; they also occur as bilateral lesions in the context of neurofibromatosis 2 (NF2), a highly penetrant, autosomal dominant disorder.

The growth rates of VSs are highly variable [1, 2], but generally increase with decreasing patient's age at onset of symptoms [3, 4]. The younger age correlates with larger tumour size [3–5]. Mutations in the *NF2* tumour suppressor gene, which is located on chromosome 22, band q11-13.1, are the cause of neurofibromatosis 2, and occur in the majority of sporadic VSs [3, 6–8]. Agnihotri et al. have identified additional point mutations in [9]. have identified additional point mutations in sporadic schwannomas, including *ARID1*, *DDR1*, *TAB3*, *ALPK2*, *CAST*, *TSC1* and *TSC2*.

Despite the huge diversity in the genes implicated in tumourigenesis, *TP53* stands out as a key tumour suppressor and the p53 transcription factor (encoded by *TP53* gene) serves a master regulator of various signaling pathways involved in this process. Phosphorylation of p53 at Ser 392 is suggested to be critical for its function [10]. A report indicated that Ser 392 phosphorylation was the more frequent modification among other possible phosphorylation sites of p53 in human tumour tissues and tumour-derived cell lines [11]. Sequence analysis of *TP53* gene in various tumours revealed point mutations in the coding region in majority of the cases. Point mutations of *TP53* have been identified in brain tumours including astrocytomas [12] and gliomas [13], but very rare in schwannomas [14–16], with one exception, where a point mutation was found in a malignantly transformed vestibular schwannoma [17]. The previous literature concerning schwannomas has used direct DNA sequencing, which detects point mutations including small intraexonic deletions/insertions; however, this technique is not able to detect deletions/duplications encompassing ≥ 1 *TP53*-exons. These lesions have been reported to be associated with several conditions, such as Li-Fraumeni syndrome [18], Breast Cancer [19] and transitional-cell carcinoma [20]. Monoh et al. Analyzed loss of heterozygosity (LOH) at the coding region of *TP53* and demonstrated no LOH in 13 informative cases [15]; however, a conflicting result has been reported in another research group, which indicated that LOH occurred at the first intron of *TP53* locus in about half of the informative cases [21]. To the best of our knowledge, no study has been made so far regarding the exonic copy number changes of *TP53* in sporadic schwannomas.

The objectives of this study were to use Multiplex ligation-dependent probe amplification (MLPA), a PCR-based semiquantitative gene dosage assay, to characterize the pattern and frequency of copy-number changes of *TP53* in patients with sporadic vestibular schwannomas and to examine the association between the *TP53* mutations, phosphorylation status of p53 protein and clinical phenotypes.

Materials and methods

Study population

A total of 44 patients who presented with a unilateral vestibular schwannoma were treated surgically in our department between March 2018 and September 2018. The duration between the onset of the first symptoms and preoperative clinic visits was 2.14 ± 2.32 years. Tumour volume of a vestibular schwannoma by magnetic resonance imaging (MRI) was calculated according to the following method [22]. Maximum tumour diameter was measured in three dimensions (transverse and longitudinal on the axial images, and vertical on the coronal images) using fine calipers. Measurements were defined as x, y, and z, respectively. Tumour volume was $xyz/2$. Tumour size was evaluated by both maximum tumour diameter and tumour volume. All patients had at least one MRI examination before surgery (Table S1, Supporting Information). For patients with MRI scans at least 6-month intervals, their tumour growth rates were calculated on the basis of the measured changes in the maximum axial diameter in millimeters per year. Informed written consent was obtained from all patients donating tissue. Five cases of vestibular nerves from vestibular neurectomy for Meniere's disease were included as controls. This study was conducted in compliance with institutional policy to protect patients' private information, and was approved by the Institutional Review Board of the ethics committee of Shanghai Jiao Tong University.

Polymerase chain reaction (PCR) and sanger sequencing

Sanger sequencing was conducted to detect microlesions in the genes. DNA extraction from the tumour (fresh and paraffin fixed) specimens was performed using the TIAN-amp Genomic DNA Kit (Tiangen Biotech, Beijing, China). The whole coding sequence and exon-intron boundaries of the genes were amplified by the polymerase chain reaction (PCR) using standard methods. The sequence data were analyzed using the Sequencer 4.9 software (GeneCode, MI, USA) and compared with the sequences of *NF2* (NM_016418) and *TP53* (NM_016418) in GeneBank. Mutations were described according to the standard nomenclature for DNA sequence changes reported by the Human Genome Variation Society (HVGs).

Multiplex ligation-dependent probe amplification analysis (MLPA) analysis

To identify exonic alterations in the *TP53* locus, we used a commercial MLPA kit for analysis (SALSA P056 TP53;

MRC-Holland, Amsterdam, The Netherlands). The probe-mix contains probes for each of the exons of *TP53*. The MLPA PCR products of test samples were separated on a 3500 Genetic Analyzer (Applied Biosystems, CA, USA), and peak heights for each PCR product were compared to a normalized average of 3 independent nerves to determine the dosage quotient (DQ) for each individual exon. A range of $0.7 < \text{DQ} < 1.2$ was considered normal, and $0.4 < \text{DQ} < 0.6$ was considered to show a heterozygous deletion. A subset of probes located on the regions of 17q 13 were also included as positive controls. Eleven reference probes were also used to detect different autosomal chromosomal regions.

Immunoblotting analysis

The tumour tissues were ultrasonicated in Cell Lysis Buffer (Beyotime, Shanghai China) containing a protease inhibitor (phenylmethanesulfonyl fluoride). Immunoblotting analyses were performed with antibodies specific for total p53 (# P6874, Sigma-Aldrich), phospho-p53-Ser 392 (#9281, Cell Signaling) and cyclinD1 (#2922, Cell Signaling). The β -actin antibody (#AA128, Beyotime) was used to ensure equal loading of total protein. The protein bands were detected using a chemiluminescence HRP substrate (Millipore). The band densities were quantified using Imager Lab Software (Bio-Rad). The band intensities of target proteins (p53, phospho-p53 and cyclinD1) in tumour specimens were expressed relative to those in the nerve controls to obtain relative values.

Cell culture and immunofluorescence

Human Schwann cells (HSCs) were purchased from ScienCell Research Laboratories (catalog no., 1700), and cultured in Schwann Cell Medium (ScienCell, Cat. No.1701). For primary cultures, schwannomas were cut to 1 mm^3 in size and digested with 0.25% trypsin as previously described [3]. Cells were then collected and re-suspended in the Schwann Cell Medium. Schwannoma cells were plated on glass slides, fixed with 4% paraformaldehyde, and then permeabilized in 0.3% Triton X-100. The glass slides were blocked with bovine serum albumin before the incubation with an anti-phospho-p53 (pSer³⁹²) antibody (# ab134190, Abcam). An Alexa-594-conjugated anti-rabbit antibody was used as the secondary antibody. The Alexa Fluor® 488 Phalloidin (# A12379, Thermo) was used to stain the F-actin cytoskeleton in schwannoma cells. Finally, the sections were nuclear counterstained with 4, 6-diamidino-2-phenylindole (DAPI, Beyotime, China).

Statistical analysis

Results are expressed as mean \pm SD ranges. Normally distribution and homogeneity of variance tests were performed on the data using SPSS statistics software (SPSS, Chicago, IL). The statistical analyses of clinical/ genetic parameters and expression/phosphorylation profiles were assessed using Chi-square test, two-tailed *t* test, bivariate correlations (Pearson's for continuous variables), and multivariate linear regression. *P* values of less than 0.05 were considered to be statistically significant.

Results

Patients

The cohort of patients consisted of 16 males (36.4%) and 28 females (63.6%) with a median age at diagnosis of 47.8 years (range from 11 to 69 years). The most frequent symptoms were hearing impairment (31 patients, 70.5%) and tinnitus (23 patients, 52.3%). Details regarding the clinical characteristics and the results of Sanger sequencing in all tumours analyzed were given in Table 1. Mutations throughout the whole coding sequence of the *NF2* gene were detected in 30 (68.2%) out of 44 cases. The majority of these mutations were truncating mutations, which were distributed along almost the entire *NF2* sequence. As expected, no point mutations of *TP53* were observed in schwannomas by Sanger sequencing.

Age-dependent multi-exon deletion mutations of the *TP53* gene in sporadic VSs

The exonic copy number changes of *TP53* in the tumour were investigated by MLPA analysis. As shown in Figs. 1 and 2, the heterozygous exonic deletion mutations of *TP53* were identified in 29/44 tumour samples (65.7%). Of these deletions, nine were single exon and twenty were multi-exons. The frequency of mutation in a specific exon was determined using the methylation values, defined as the number of tumour mutated /the number of tumour tested. These mutations were more likely to occur in exons 9, 1, 6, with respective frequencies of 50.0%, 45.5%, and 45.5%. Exons 2, 4 and 11 had lower mutation frequencies (27. 2%, 25.0%, and 2.3%, respectively), and none of the mutations were found in exons 7 and 10.

An overview regarding clinical and genetic characteristics of mutated ($n = 29$) and non-mutated ($n = 15$) patients is shown in Table 2. There was no predilection for sex, tumour side or tumour type of the lesion in both groups. Notably, we found that patients with mutant *TP53* had an earlier age at diagnosis (mean 25.4 ± 9.5 vs. 55.2 ± 12.1 years, $P = 0.001$)

Table 1 Clinical and genetic information of patients with sporadic vestibular schwannomas

Case	Gender	Age (years)	Side	Diameter (mm)	Volume (cm ³)	NF2 gene point mutation	Sequence alteration		Codon	Consequence	TP53 gene point mutation
							Exon				
T360	M	22	R	22	3.0	E3	c.331C>T	p.Q111X	Nonsense	None	
T410	F	21	L	35	8.8	E3	c.361_363+25del128bp	/	Splice donor site	None	
T411	M	52	R	28	6.1	E6	c.586 C>T	p.R196X	Nonsense	None	
T412	F	29	R	30	11.1	/	None	None	None	None	
T344	M	43	L	18	2.7	E2	c.169C>T	p.Y57X	Nonsense	None	
T416	M	50	L	29	7.2	E12	c.1228 C>T	p.Q410X	Nonsense	None	
T350	M	40	R	22	2.3	E6	c.586 C>T	p.R196X	Nonsense	None	
T351	F	69	L	25	1.3	E15	c.1609delG	p.E537X	Nonsense	None	
T353	F	64	R	25	5.0	/	None	None	None	None	
T354	F	47	R	25	5.7	E5	c.460delG	p.D154TfsX18	Frameshift	None	
T355	F	55	L	20	3.2	E12	c.1252_1268del117bp	p.R418AfsX17	Frameshift	None	
T361	M	64	L	30	6.3	/	None	None	None	None	
T363	F	66	L	15	0.5	E9	c.883delC	p.L127X	Nonsense	None	
T364	F	75	R	25	3.3	E7	c.620_632del13bp	p.L295LfsX14	Frameshift	None	
T365	M	66	R	33	9.8	E9	c.813delT	p.F271TfsX23	Frameshift	None	
T368	M	51	L	47	23.1	E12	c.1165delC	p.Q389RfsX35	Frameshift	None	
T370	F	35	L	15	0.5	E8	c.737delC	p.P246LfsX3	Frameshift	None	
T377	F	63	R	28	6.1	E6	c.573delG	p.W191CfsX16	Frameshift	None	
T378	F	22	L	23	3.9	/	None	None	None	None	
T379	M	52	L	15	1.7	E10	c.962_983del22bp	p.M321RfsX15	Frameshift	None	
T380	F	22	L	30	10.9	E3	c.334G>T	p.E12X	Nonsense	None	
T381	M	35	R	23	4.1	E9	c.865A>T	p.K289X	Nonsense	None	
T382	F	52	R	30	7.3	E5	c.488 T>A	p.F163X	Nonsense	None	
T384	F	52	R	33	10.6	E3	c.241-1 G>A	/	Splice acceptor site	None	
T385	F	11	R	25	5.0	E2	c.169C>T	p.Y57X	Nonsense	None	
T387	F	65	R	26	5.0	E1	c.31_34 del TTCA	p.F11AfsX13	Frameshift	None	
T388	F	43	R	40	22.6	E5	c.448-2 G>T	/	Splice acceptor site	None	
T391	F	49	R	35	13.6	E9	c.848DelT	p.F283SfsX11	Frameshift	None	
T400	F	39	R	30	7.3	E11	c.1121+1DelGTG	/	Splicing donor site	None	
T401	F	64	R	30	9.1	E7	c.622_623 delCT	p.L208EfsX17	Frameshift	None	
T402	M	66	R	20	1.9	E14	c.1447-1 G>A	/	Splice acceptor sit	None	
T403	F	43	L	10	0.3	/	None	None	None	None	
T404	F	16	R	32	13.8	E6	c.564delT	p.I188fsX19	Frameshift	None	
T405	F	36	L	25	3.3	/	None	None	None	None	
T408	M	40	R	19	0.9	/	c.599+1 G>A	None	Splicing donor site	None	

Table 1 (continued)

Case	Gender	Age (years)	Side	Diameter (mm)	Volume (cm ³)	NF2 gene point mutation		Codon	Consequence	TP53 gene point mutation
						Exon	Sequence alteration			
T420	F	40	L	27	6.0	E13	c.1411A>T	p.K171X	Nonsense	None
T421	F	64	R	10	0.2	/	None	None	None	None
T422	M	54	L	15	1.0	E13	c.1366C>T	p.Q456X	Nonsense	None
T424	M	61	R	16	1.1	/	None	None	None	None
T425	M	46	R	26	10.7	E4	c.447+2T>C	/	Splice donor site	None
T426	M	55	L	35	21	E15	c.1604T>C	p.L353P	Missense	None
T406	F	55	L	12	1.6	/	None	None	None	None
T366	F	45	R	30	9.0	/	None	None	None	None
T392	F	47	R	30	9.7	/	None	None	None	None

compared to patients with no *TP53* mutations, and mutation carriers were more likely to suffer from larger tumours (maximum diameter, mean 26.8 ± 7.4 vs. 22.4 ± 8.9 mm, $P = 0.120$; volume, mean 7.0 ± 5.6 vs. 5.6 ± 6.0 cm², $P = 0.460$). The mutation index (MI), defined as the number of *TP53*-exons mutated/ the number of *TP53*-exons tested in a tumour, showed a negative correlation with the patient's age (Fig. 3a; Spearman's rho = -0.35, $P = 0.02$). Moreover, there were a significant positive correlation between MI and both maximum tumour diameter (Fig. 3b; Spearman's rho = 0.42, $P = 0.002$) and tumour volume (Fig. 3c; Spearman's rho = 0.34, $P = 0.024$). Younger the age of patients or large tumor size is known to be associated with higher growth rate of VSs [3–5]. The growth rates of three *TP53*-mutated patients (T351, T360 and T380; marked in red; Table S1) was 3.7 ± 3.2 mm/ year, while the growth rates of three non-mutated patients (T365, T422 and T406; marked in green) was 0.63 ± 1.1 mm/ year. These patients underwent MRI studies at least 6-month intervals. Although the sample size was very small, the data showed that *TP53*-mutated tumours grow faster than non-mutated counterparts ($p = 0.087$). Thus, exonic deletion mutations of *TP53* may play a role in the acceleration of tumour growth, thus contributing to an early age at symptom in patients with sporadic VSs.

Phosphorylation patterns of p53 in correlation with mutational status of *TP53* in schwannomas

Function of the wild-type p53 protein is known to be dependent on the conformation and phosphorylation of its serine residues, Ser 392 in particular [10]. High levels of phospho-Ser392-p53 have been observed in tumours with mutant p53 [23]. Next, we investigated if *TP53* mutations influenced Ser 392 phosphorylation of p53 in schwannomas. As shown in Fig. 4a–c, the levels of total/phosphorylated p53 and its downstream cyclin D1 varied between the 26 cases of tumour samples. The band intensities of target proteins in tumours were expressed relative to those in the nerve controls to obtain relative grey scale values. As indicated in Fig. 4d, the phosphorylation levels of p53 were changed in positive correlation to its total protein levels ($r^2 = 0.6$, $P < 0.001$), suggesting that p53 was frequently phosphorylated at Ser 392 in schwannomas. There was a highly negative correlation between the patient's age and levels of both total and phosphorylated p53 ($r^2 = 0.21$, $P = 0.018$; $r^2 = 0.27$, $P = 0.006$; respectively). The mutation index (MI) and patient's age were also correlated ($r^2 = 0.29$, $P = 0.043$). Thus, an age-dependent phosphorylation pattern of p53 in correlation with its mutation status was suggested in schwannomas. No statistically significant correlation was observed between the level of cyclin D1 and patient's age (Spearman's rho = 0.08, $P = 0.71$). As shown in Fig. 4a–c,

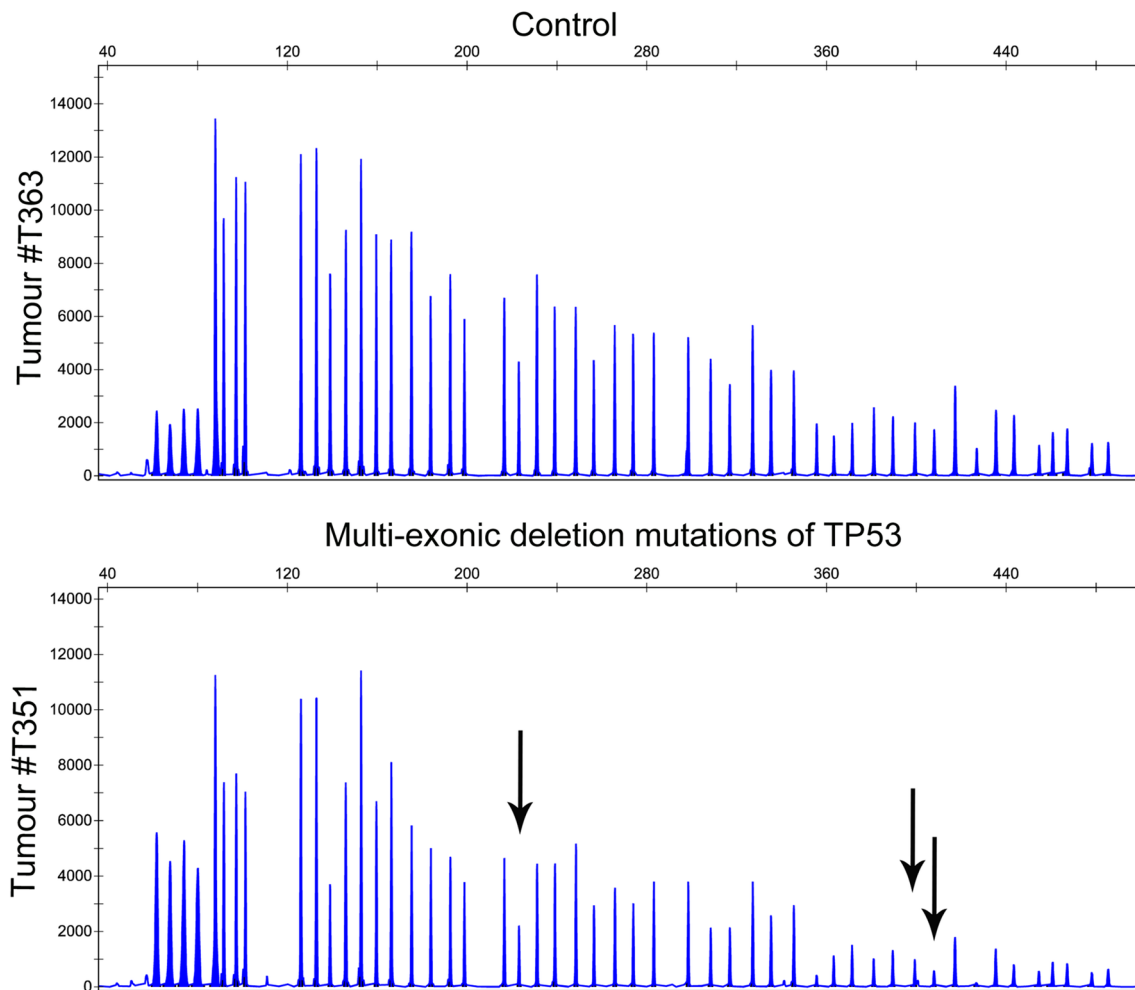


Fig. 1 MLPA analyses of copy number changes of *TP53* in schwannomas. In the graph, the y-coordinate represented the Dosage Quotient (DQ) and $0.4 < DQ < 0.6$ was considered to have a heterozygous

deletion. MLPA showed one tumour (# T363) with normal *TP53* alleles and one tumour (# T351) with heterozygous deletions of exon 1, 6, and 9 at the *TP53* locus

four cases (T364, 384, 406 and 402) exhibited no marked levels of total/ phosphorylated p53; these patients were above 50 years of age and 3 out (75%) of them had no *TP53* mutations. By contrast, an appreciable amount of phospho-Ser392-p53 was observed in five mutated tumours (T381, 378, 424, 385 and 408), most of which were from young patients with an average age of 33.8 years. Altogether, these findings indicated that Ser 392 phosphorylation of p53 in correlation with its mutation status was more likely to occur in young patients.

Nuclear accumulation of p53 protein associated with its Ser 392 phosphorylation in mutated tumours

It was reported that the modification of Ser 392 could stabilize p53 by blocking the nuclear export of p53, thus inhibiting proteasome-mediated degradation via MDM2 [24]. To

characterize the subcellular localization of phospho-Ser392-p53 in schwannomas, we performed fluorescence analyses of cultures from one mutated tumour (#T381) with hyperphosphorylated p53, one non-mutated tumour (#T406) with underphosphorylated p53 and human Schwann cells (HSCs). The phospho-Ser392-p53 was predominantly stained in the nucleus of HSCs (Fig. 5, upper). The diffuse nuclear and cytoplasmic staining of phospho-Ser392-p53 was observed in the schwannoma cultures # T406 (Fig. 5, center). Additionally, this finding was consistent with a previous study showing a diffuse pattern of p53 staining with a p53-specific antibody in schwannomas [25]. By contrast, schwannoma cells from tumour # T381 exhibited strong localization of phospho-Ser392-p53 to the nucleus (Fig. 5, lower). Thus, we demonstrated an enhanced stability of phospho-Ser392-p53, which was characterized by nuclear accumulation in schwannoma cultures with p53 mutations.

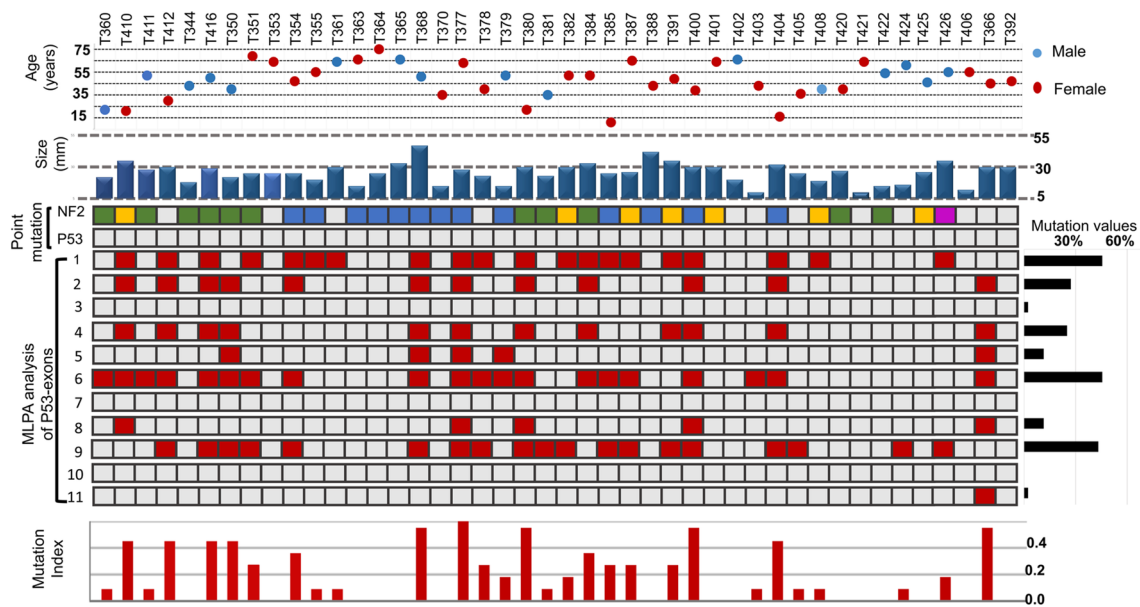


Fig. 2 Clinical and genetic characteristics of patients with sporadic VSs aged from 21 to 65 years. The clinical parameters including the age at diagnosis, gender and tumour size were present in the upper panel. Point mutations in the *NF2* gene were demonstrated in the

majority of tumours, whereas no point mutations of *TP53* were found by direct sequencing. The mutation index (MI) for each tumour (*bottom*) and the mutation frequencies (indicated as ‘mutation values’; *right*) for each exon of *TP53* were shown

Table 2 Clinical characteristics in patients with or without exonic deletion mutations of *TP53*

Tumor characteristics	Mutated (n=29)	Non-mutated (n=15)	P value	Statistical methods
Mean age (years)	25.4 ± 9.5	55.2 ± 12.1	0.001	Two tailed t test
Gender				
Male	11	5	0.117	χ^2 test
Female	18	10		
Tumour side				
Right side	17	9	0.577	χ^2 test
Left side	12	6		
Tumour type				
Solid	23	11	0.846	χ^2 test
Cystic	6	4		
Tumour volume (cm ²)	7.0 ± 5.6	5.6 ± 6.0	0.460	Two tailed t test
Size (mm)	26.8 ± 7.4	22.4 ± 8.9	0.120	Two tailed t test
Stage 2 (1–15 mm)	2	6		
Stage 3 (16–30 mm)	21	7		
Stage 4 (31–40 mm)	4	1		
Stage 5 (> 40 mm)	2	1		
NF2 alterations	22 (75.9%)	10 (66.7%)	0.722	χ^2 test
Nonsense	8	3		
Frameshift	8	5		
Splicing site	5	2		
Missense	1	0		

Discussion

Sequence analysis have revealed that the point mutations

of *TP53* are the most frequent alterations in the transitional stage during which a tumour progresses; these mutations are distributed in all coding exons of *TP53* [26]. Our results confirmed the previous reports on the absence of point

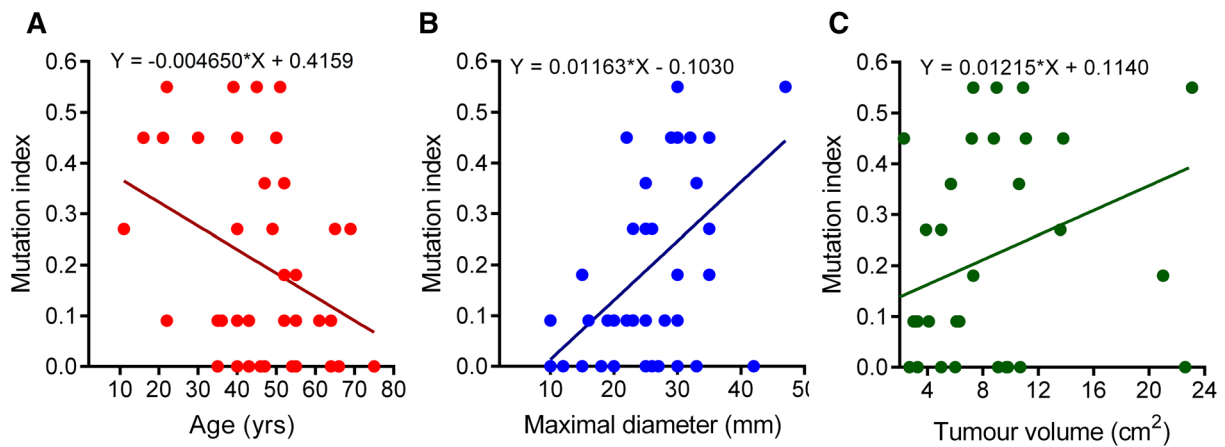


Fig. 3 Correlation between the mutation index of *TP53* and both tumour size and patient's age. The mutation index showed a significant correlation with the patient's age (a) and tumour size, which was measured by the maximal tumour diameter (b) and tumour volume (c)

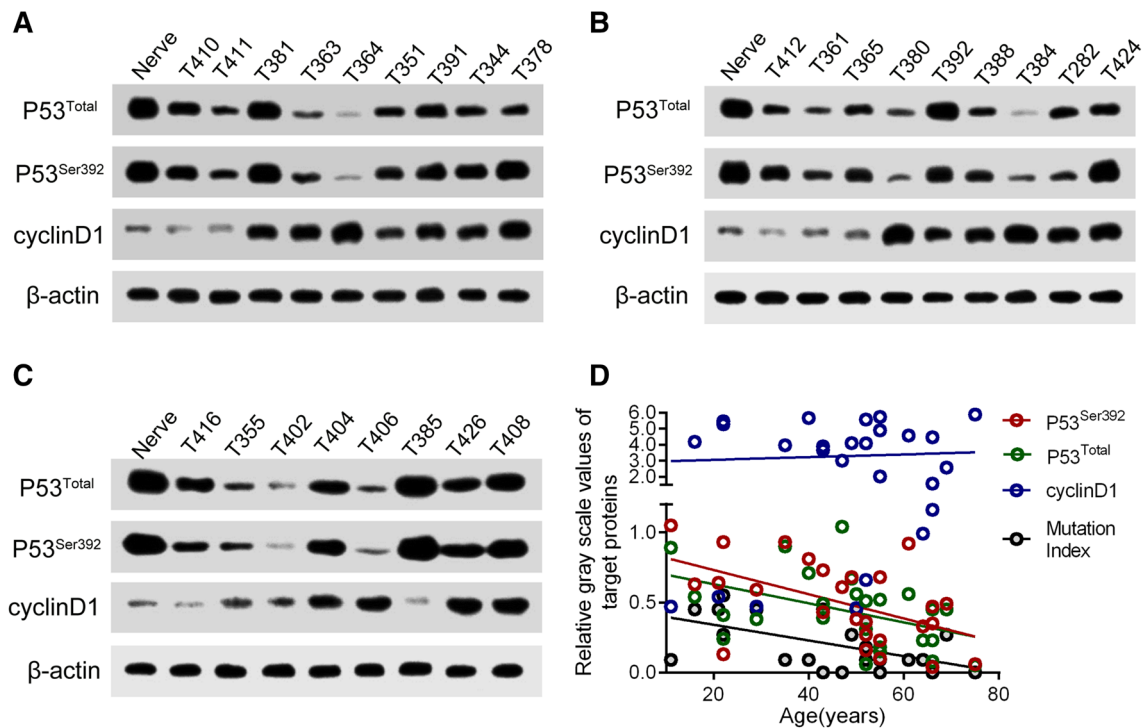


Fig. 4 Expression and phosphorylation status of p53 protein in schwannomas with and without *TP53* mutations. a–c The expression levels of cyclinD1 and both total and phosphorylated p53 were investigated by immunoblotting analysis. d The band intensities of target

proteins in tumours were expressed relative to those in the nerve controls to obtain relative grey scale values. The correlations of the patient's age with both relative grey scale values and mutation index of *TP53* were analyzed

mutations at *TP53* locus in schwannomas; instead exonic deletion mutations were noted in 64% of tumours. Unlike the malignancies where point mutations of *TP53* frequently occur in exons 5 through 8 [26], the exonic deletion mutations in schwannomas were demonstrated to be clustered within exons 9, 6 and 1. There are several reports on the

role of *TP53* alterations in relation to the clinical/pathological features of tumours. Niederacher et al. correlated LOH [27], correlated LOH of *TP53* with younger patients and a higher histological grading in sporadic endometrial cancer. *NF2-TP53*-double mutant mice exhibited an increased predisposal to neoplasms compared with each of the single

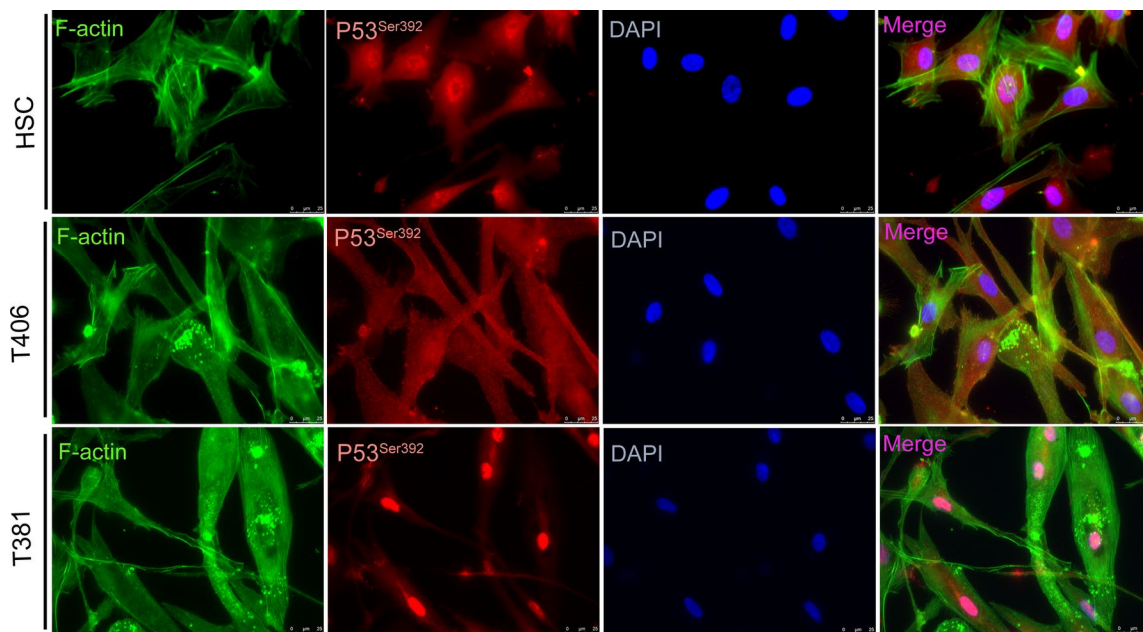


Fig. 5 The subcellular localization of Ser 392 phosphorylated p53 in schwannoma cultures and human Schwann cells (HSCs). Phospho-Ser392-p53 was predominantly stained in the nucleus of HSCs (*upper*). The diffuse nuclear and cytoplasmic staining of phospho-

Ser392-p53 was observed in the schwannoma cultures # T406 (*center*). By contrast, schwannoma cells from tumour # T381 exhibited strong localization of phospho-Ser392-p53 to the nucleus (*lower*)

mutant mice [28]. In a cohort of meningiomas, whose tumourigenesis was also related to *NF2* mutation, *TP53* polymorphism increased the risk of tumour progression [29]. Consistent with these studies, we found that schwannomas with exonic deletion mutations of *TP53* exhibited rapid growing behaviors including larger tumour size and younger patient's age. It has been reported that the wild-type p53 functions optimally when it binds to DNA as a tetramer; the wild type and mutant p53 can form hetero-tetramers of attenuated activity, via their tetramerization domains [30, 31]. In this mechanism, the severer phenotype of *TP53*-mutated schwannomas might be explained by the fact that the mutant p53 could disturb a functional tetramer and was therefore able to override wild-type p53 tumor suppressor activity.

Phosphorylation of p53 at Ser 392 can activate the specific DNA binding function of p53, presumably by stabilizing its tetramer [10]. Ser 392 phosphorylation of mutant p53 protein might promote its dominant negative effects through hetero-oligomerization, thereby contributing to the aggressive behaviors of tumours [32]. An increased percentage of the Ser 392 phosphorylated form of p53 was found only in histological high-grade gliomas (grades III and IV). On the contrary, a lower percentage of the Ser 392 phosphorylated form of p53 was present in histological low-grade gliomas, meningiomas and other brain tumour types [33]. In present study we suggested that hyperphosphorylated p53 appeared to occur more often in mutated schwannomas

in young patients. Down-regulation of p53 protein is commonly seen in schwannoma tissues and in vitro cultures [25, 34]; these studies showed that p53 was abnormally sequestered in the cytoplasm of p53-deficient schwannomas. It has been suggested that merlin neutralizes the inhibitory effect of MDM2 on p53 [35], and, merlin loss by *NF2* mutation confers an enhanced nuclear accumulation of MDM2 and thereby induces nuclear export of p53 for degradation in schwannomas [25]. We show that p53 deficiency along with its hypophosphorylation at Ser 392 is frequently observed in schwannomas with no *TP53* mutation. In addition, some studies have reported a subset of schwannomas characterized by p53 overexpression [14, 21, 25]. This current study suggests that this deregulation may be independent of merlin loss and linked to the occurrence of exonic deletion mutation of *TP53*. It is possible that the deficiency of wild-type p53 due to merlin loss by *NF2* mutations may play a role on the early biological changes during schwannoma tumourigenesis. The exonic deletion mutation of *TP53* may occur as a second genetic hit, leading to the phosphorylation and stabilization of p53 protein with attenuated tumour-suppression activity, thus promoting tumour growth and resulting in early clinical symptoms.

Using several lines of investigation, therefore, our studies propose a connection between the mutation pattern of *TP53* and phosphorylation status of p53 and clinical characteristics in human sporadic VSs. These studies deserve further investigations to uncover mechanisms underlying

the biological effect of *TP53* mutation characterized by Ser 392 phosphorylation of p53 on the growth of schwannoma. Unlike genetic mutations, phosphorylation is a reversible process, and thus countering the effects of Ser 392 phosphorylation of p53 protein could be a novel target for therapeutic purposes to reduce the growth of schwannomas.

Acknowledgements This research was funded by the National Natural Science Foundation of China (Grant No. 81800898 to Hongsai Chen, No. 81670919 and No. 81870713 to Zhaoyan Wang, No. 81570906 to Hao Wu, No. 81700900 to Weidong Zhu and No. 81600815 to Yongchuan Chai).

Compliance with ethical standards

Conflict of interest The authors declare that they have no competing interests.


References

- Zhu W, Chen H, Jia H, Chai Y, Yang J, Wang Z, Wu H (2018) Long-term hearing preservation outcomes for small vestibular schwannomas: retrosigmoid removal versus observation. *Otol Neurotol* 39(2):e158–e165. <https://doi.org/10.1097/MAO.0000000000001684>
- Huang X, Caye-Thomasen P, Stangerup SE (2013) Spontaneous tumour shrinkage in 1261 observed patients with sporadic vestibular schwannoma. *J Laryngol Otol* 127(8):739–743. <https://doi.org/10.1017/S0022215113001266>
- Chen H, Xue L, Wang H, Wang Z, Wu H (2017) Differential NF2 gene status in sporadic vestibular schwannomas and its prognostic impact on tumour growth patterns. *Sci Rep* 7(1):5470. <https://doi.org/10.1038/s41598-017-05769-0>
- Chen H, Zhang X, Zhang Z, Yang T, Wang Z, Wu H (2014) The role of NF2 gene mutations and pathogenesis-related proteins in sporadic vestibular schwannomas in young individuals. *Mol Cell Biochem* 392(1–2):145–152. <https://doi.org/10.1007/s11010-014-2011-9>
- Bull JG, Lipson AC, Martin AJ (2006) Giant vestibular schwannoma in a 12-year-old girl. *Pediatr Neurosurg* 42(5):338–340. <https://doi.org/10.1159/000094076>
- Hadfield KD, Smith MJ, Urquhart JE, Wallace AJ, Bowers NL, King AT, Rutherford SA, Trump D, Newman WG, Evans DG (2010) Rates of loss of heterozygosity and mitotic recombination in NF2 schwannomas, sporadic vestibular schwannomas and schwannomatosis schwannomas. *Oncogene* 29(47):6216–6221. <https://doi.org/10.1038/onc.2010.363>
- Bian LG, Tirakotai W, Sun QF, Zhao WG, Shen JK, Luo QZ (2005) Molecular genetics alterations and tumour behavior of sporadic vestibular schwannoma from the People's Republic of China. *J Neurooncol* 73(3):253–260. <https://doi.org/10.1007/s11060-004-5176-3>
- Lassaletta L, Torres-Martín M, Peña-Granero C, Roda JM, Santa-Cruz-Ruiz S, Castresana JS, Gavilan J, Rey JA (2013) NF2 genetic alterations in sporadic vestibular schwannomas: clinical implications. *Otol Neurotol* 34(7):1355–1361. <https://doi.org/10.1097/MAO.0b013e318298ac79>
- Agnihotri S, Jalali S, Wilson MR, Danesh A, Li M, Klironomos G, Krieger JR, Mansouri A, Khan O, Mamatjan Y, Landon-Brace N, Tung T, Dowar M, Li T, Bruce JP, Burrell KE, Tonge PD, Alamsahebpour A, Kriscsek B, Agarwalla PK, Bi WL, Dunn IF, Beroukheim R, Fehlings MG, Bril V, Pagnotta SM, Iavarone A, Pugh TJ, Aldape KD, Zadeh G (2016) The genomic landscape of schwannoma. *Nat Genet* 48(11):1339–1348. <https://doi.org/10.1038/ng.3688>
- Sakaguchi K, Sakamoto H, Lewis MS, Anderson CW, Erickson JW, Appella E, Xie D (1997) Phosphorylation of serine 392 stabilizes the tetramer formation of tumour suppressor protein p53. *Biochemistry* 36(33):10117–10124. <https://doi.org/10.1021/bi970759w>
- Minamoto T, Buschmann T, Habelhah H, Matusевич E, Tahara H, Boerresen-Dale AL, Harris C, Sidransky D, Ronai Z (2001) Distinct pattern of p53 phosphorylation in human tumours. *Oncogene* 20(26):3341–3347. <https://doi.org/10.1038/sj.onc.1204458>
- Gutmann DH, James CD, Poyhonen M, Louis DN, Ferner R, Guha A, Hariharan S, Viskochil D, Perry A (2003) Molecular analysis of astrocytomas presenting after age 10 in individuals with NF1. *Neurology* 61(10):1397–1400. <https://doi.org/10.1212/WNL.61.10.1397>
- Gillet E, Alentorn A, Doukouré B, Mundwiler E, van Thuijl HF, Reijneveld JC, Medina JA, Liou A, Marie Y, Mokhtari K, Hoang-Xuan K, Sanson M, Delattre JY, Idhah A (2014) TP53 and p53 statuses and their clinical impact in diffuse low grade gliomas. *J Neurooncol* 118(1):131–139. <https://doi.org/10.1007/s11060-014-1407-4>
- Chen Y, Wang ZY, Wu H (2015) P14ARF deficiency and its correlation with overexpression of p53/MDM2 in sporadic vestibular schwannomas. *Eur Arch Otorhinolaryngol* 272(9):2227–2234. <https://doi.org/10.1007/s00405-014-3135-y>
- Monoh K, Ishikawa K, Yasui N, Mineura K, Andoh H, Togawa K (1998) p53 tumour suppressor gene in acoustic neuromas. *Acta Otolaryngol Suppl* 537:11–15. <https://doi.org/10.1080/00016489850182288>
- Ohgaki H, Eibl RH, Schwab M, Reichel MB, Mariani L, Gehring M, Petersen I, Höll T, Wiestler OD, Kleihues P (1993) Mutations of the p53 tumour suppressor gene in neoplasms of the human nervous system. *Mol Carcinog* 8(2):74–80. <https://doi.org/10.1002/mc.2940080203>
- Yanamadala V, Williamson RW, Fusco DJ, Eschbacher J, Weiskopf P, Porter RW (2013) Malignant transformation of a vestibular schwannoma after gamma knife radiosurgery. *World Neurosurg* 79(3–4):593. <https://doi.org/10.1016/j.wneu.2012.03.016>
- Shlien A, Baskin B, Achatz MI, Stavropoulos DJ, Nichols KE, Hudgins L, Morel CF, Adam MP, Zhukova N, Rotin L, Novokmet A, Druker H, Shago M, Ray PN, Hainaut P, Malkin D (2010) A common molecular mechanism underlies two phenotypically distinct 17p13.1 microdeletion syndromes. *Am J Hum Genet* 87(5):631–642. <https://doi.org/10.1016/j.ajhg.2010.10.007>
- Mouchawar J, Korch C, Byers T, Pitts TM, Li E, McCredie MR, Giles GG, Hopper JL, Southey MC (2010) Population-based estimate of the contribution of TP53 mutations to subgroups of early-onset breast cancer: Australian Breast Cancer Family Study. *Cancer Res* 70(12):4795–4800. <https://doi.org/10.1158/0008-5472.CAN-09-0851>
- Bazrafshani MR, Nowshadi PA, Shirian S, Daneshbod Y, Nabipour F, Mokhtari M, Hosseini F, Dehghan S, Saeedzadeh A, Mosayebi Z (2016) Deletion/duplication mutation screening of TP53 gene in patients with transitional cell carcinoma of urinary bladder using multiplex ligation-dependent probe amplification. *Cancer Med* 5(2):145–152. <https://doi.org/10.1002/cam4.561>
- Dayalan AH, Jothi M, Keshava R, Thomas R, Gope ML, Doddaballapur SK, Somanna S, Praharaj SS, Ashwathnarayanarao CB, Gope R (2006) Age dependent phosphorylation and deregulation of p53 in human vestibular schwannomas. *Mol Carcinog* 45(1):38–46. <https://doi.org/10.1002/mc.20150>
- Nakamura H, Jokura H, Takahashi K, Boku N, Akabane A, Yoshimoto T (2000) Serial follow-up MR imaging after gamma knife

- radiosurgery for vestibular schwannoma. *AJNR Am J Neuroradiol* 21(8):1540–1546
23. Matsumoto M, Furihata M, Ohtsuki Y (2006) Posttranslational phosphorylation of mutant p53 protein in tumor development. *Med Mol Morphol* 39(2):79–87. <https://doi.org/10.1007/s00795-006-0320-0>
 24. Kim YY, Park BJ, Kim DJ, Kim WH, Kim S, Oh KS, Lim JY, Kim J, Park C, Park SI (2004) Modification of serine 392 is a critical event in the regulation of p53 nuclear export and stability. *FEBS Lett* 572(1–3):92–98. <https://doi.org/10.1016/j.febslet.2004.07.014>
 25. Chen H, Xue L, Huang H, Wang H, Zhang X, Zhu W, Wang Z, Wang Z, Wu H (2018) Synergistic effect of Nutlin-3 combined with MG-132 on schwannoma cells through restoration of merlin and p53 tumour suppressors. *EBioMedicine* 36:252–265. <https://doi.org/10.1016/j.ebiom.2018.09.042>
 26. Olivier M, Eeles R, Hollstein M, Khan MA, Harris CC, Hainaut P (2002) The IARC TP53 database: new online mutation analysis and recommendations to users. *Human Mutat* 19(6):607–614. <https://doi.org/10.1002/humu.10081>
 27. Niederacher D, An HX, Camrath S, Dominik SI, Göhring UJ, Oertel A, Grass M, Hantschmann P, Lordnejad MR, Beckmann MW (1998) Loss of heterozygosity of BRCA1, TP53 and TCRD markers analysed in sporadic endometrial cancer. *Eur J Cancer* 34(11):1770–1776. [https://doi.org/10.1016/S0959-8049\(98\)00270-6](https://doi.org/10.1016/S0959-8049(98)00270-6)
 28. Robanus-Maandag E, Giovannini M, van der Valk M, Niwa-Kawakita M, Abramowski V, Antonescu C, Thomas G, Berns A (2004) Synergy of Nf2 and p53 mutations in development of malignant tumours of neural crest origin. *Oncogene* 23(39):6541–6547. <https://doi.org/10.1038/sj.onc.1207858>
 29. Chang Z, Guo CL, Ahronowitz I, Stemmer-Rachamimov AO, MacCollin M, Nunes FP (2009) A role for the p53 pathway in the pathology of meningiomas with NF2 loss. *J Neurooncol* 91(3):265–270. <https://doi.org/10.1007/s11060-008-9721-3>
 30. Joerger AC, Fersht AR (2007) Structure-function-rescue: the diverse nature of common p53 cancer mutants. *Oncogene* 26(15):2226–2242. <https://doi.org/10.1038/sj.onc.1210291>
 31. Junk DJ, Vrba L, Watts GS, Oshiro MM, Martinez JD, Futscher BW (2008) Different mutant/wild-type p53 combinations cause a spectrum of increased invasive potential in nonmalignant immortalized human mammary epithelial cells. *Neoplasia* 10(5):450–461. <https://doi.org/10.1593/neo.08120>
 32. Furihata M, Kurabayashi A, Matsumoto M, Sonobe H, Ohtsuki Y, Terao N, Kuwahara M, Shuin T (2002) Frequent phosphorylation at serine 392 in over expressed p53 protein due to missense mutation in carcinoma of the urinary tract. *J pathol* 197(1):82–88. <https://doi.org/10.1002/path.1082>
 33. Rohini K, Mathivanan J, Prabhu PD, Subbakrishna DK, Gope ML, Chandramouli BA, Sampath S, Anandh B, Gope R (2007) Loss of heterozygosity of the p53 gene and deregulated expression of its mRNA and protein in human brain tumours. *Mol Cell Biochem* 300(1–2):101–111. <https://doi.org/10.1007/s11010-006-9374-5>
 34. Ammoun S, Schmid MC, Zhou L, Hilton DA, Barczyk M, Hanemann CO (2015) The p53/mouse double minute 2 homolog complex deregulation in merlin-deficient tumours. *Mol Oncol* 9(1):236–248. <https://doi.org/10.1016/j.molonc.2014.08.005>
 35. Kim H, Kwak NJ, Lee JY, Choi BH, Lim Y, Ko YJ, Kim YH, Huh PW, Lee KH, Rha HK, Wang YP (2004) Merlin neutralizes the inhibitory effect of Mdm2 on p53. *J Biol Chem* 279(9):7812–7818. <https://doi.org/10.1074/jbc.M305526200>

Publisher's Note Springer Nature remains neutral with regard to jurisdictional claims in published maps and institutional affiliations.

Affiliations

Hongsai Chen^{1,2,3,4} · He Huang^{1,2,3} · Jingjing Zhao^{1,2,3} · Zhigang Wang^{1,2,3} · Mengling Chang⁵ · Lu Xue^{1,2,3} · Weidong Zhu^{1,2,3} · Yongchuan Chai^{1,2,3} · Gen Li^{1,2,3} · Zhaoyan Wang^{1,2,3}  · Hao Wu^{1,2,3}

¹ Department of Otolaryngology Head & Neck Surgery, The Ninth People's Hospital, School of Medicine, Shanghai Jiao Tong University, No. 639, Zhi-Zao-Ju Road, Shanghai 200011, China

² Ear Institute, School of Medicine, Shanghai Jiao Tong University, Shanghai, China

³ Shanghai Key Laboratory of Translational Medicine On Ear and Nose Diseases, Shanghai, China

⁴ Shanghai Institute of Precision Medicine, The Ninth People's Hospital, School of Medicine, Shanghai Jiao Tong University, Shanghai, China

⁵ Department of Burn and Plastic Surgery, Shanghai Jiao Tong University, School of Medicine, Rui Jin Hospital, Shanghai, China